Utilization of Sewage-Sludge-Derived Hydrochars toward Efficient Cocombustion with Different-Rank Coals: Effects of Subcritical Water Conversion and Blending Scenarios

ARTICLE *in* ENERGY & FUELS · SEPTEMBER 2014

Impact Factor: 2.79 · DOI: 10.1021/ef501386g

4 AUTHORS, INCLUDING:

Chao He
Nanyang Technological University
12 PUBLICATIONS **110** CITATIONS
SEE PROFILE

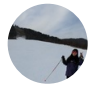

Ke Wang
London South Bank University
297 PUBLICATIONS **6,084** CITATIONS
SEE PROFILE

energy&fuels

Article

pubs.acs.org/EF

Utilization of Sewage-Sludge-Derived Hydrochars toward Efficient Cocombustion with Different-Rank Coals: Effects of Subcritical Water Conversion and Blending Scenarios

Chao He,*[,†,‡] Ke Wang,[§] Yanhui Yang,[∥] and Jing-Yuan Wang*[,†,‡]

[†]Residues and Resource Reclamation Centre, Nanyang Environment and Water Research Institute, Nanyang Technological University, 1 Cleantech Loop, Singapore 637141, Singapore

[‡]Division of Environmental and Water Resources Engineering, School of Civil and Environmental Engineering, Nanyang Technological University, 50 Nanyang Avenue, Singapore 639798, Singapore

[§]School of Municipal and Environmental Engineering, Harbin Institute of Technology, 73 Huanghe Road, Harbin, Heilongjiang 150090, China

[∥]School of Chemical and Biomedical Engineering, Nanyang Technological University, 50 Nanyang Avenue, Singapore 639798, Singapore

ABSTRACT: In the absence of prior drying, dewatered sewage sludge (DSS) was directly converted to hydrochars with superior fuel characteristics in subcritical water. Hydrochar derived at 320 °C and 12.0 MPa (SHC-320) was screened for systematic cocombustion with different-rank coals. The results suggest that SHC-320 reduced the activation energy of the blends and altered the main combustion profiles. Meanwhile, blending of SHC-320 induced greater heat loss for higher-rank coals, whereas a higher portion of SHC-320 further improved the ignition reactivity of high-rank coal blends. In the high-temperature region, the value of the pre-exponential factor increased with increasing coal/SHC-320 ratio, resulting in more intense synergistic effects in blends. At a low coal/SHC-320 ratio (30:70), intense antisynergistic effects occurred in cocombustion with low- or high-rank coals. As a result of distinct synergistic interactions, cocombustion with moderate-rank coal achieved the best combustion efficiency among the blends. These findings benefit efficient utilization of DSS as a hydrochar solid fuel in existing cofiring power plants.

1. INTRODUCTION

With rapid urbanization and the increasingly stringent regulations on the quality of effluents, the generation of sewage sludge (SS) from wastewater treatment plants is soaring globally.[1] In general, SS is rich in nutrients (nitrogen, phosphorus, and potassium) and organic matter that is mainly composed of proteins, carbohydrates, and small amounts of lipids and lignin. Thus, SS could be considered as biomass with a higher heating value (HHV) comparable to that of lignite. Nevertheless, pollutants present in SS, such as heavy metals, pathogens, and persistent organic pollutants, may endanger the environment and human health. Thus, appropriate treatment and efficient utilization of SS is imperative. Given the refractory pollutants and desirable calorific value in SS, thermochemical processes (i.e., pyrolysis, gasification, and combustion) have been widely applied as efficient technologies for final disposal and energy recovery from SS.[2] However, the high moisture content (approximately 70−80 wt %) in dewatered sewage sludge (DSS) has hindered its further utilization as a solid fuel. Because of a huge amount of vicinal and bound water therein and the relatively high latent heat of water, conventional mechanical and thermal drying are energy-intensive.[3] More recently, some novel energy-saving drying technologies have been developed, such as solvent-aided dewatering[3] and the combination of hydrothermal pretreatment and convective drying.[4]

In order to reduce coal consumption by substituting a certain amount of coal with SS, cocombustion of SS and coals has been explored.[5] However, the fuel characteristics of SS and coals are quite different,[6] and the high content of volatile matter (VM) in SS could result in unstable flame. Thus, the cocombustion performance of dried SS and coals may be considerably affected.[7] The presence of high nitrogen and sulfur contents in SS may cause high emissions of NO_x and SO_x, which could increase the cost for flue gas cleaning. Hence, it is essential to upgrade the fuel quality of SS to meet the requirements for cofiring purposes based on current infrastructures.[8] Hydrothermal carbonization of SS has been applied to produce solid fuels of better quality, termed hydrochar, for energy generation without prior drying.[7,9,10] Apart from the upgraded HHV and fuel ratio for hydrochar via dehydration and decarboxylation, it has also been found that N and S precursors in hydrochar can be significantly reduced during hydrothermal carbonization.[10] Moreover, the quality of emissions from combustion of SS-derived hydrochars (SHCs) can be further improved. Parshetti et al.[7] reported that emissions of CO and CH_4 were mitigated through cocombustion of SHC and low-rank coal. During the combustion of hydrothermally pretreated sludge, as a result of the transformation of protein structure via hydrothermal treatment, interactions between NO and NH_3 were facilitated, allowing NO emissions to be reduced.[9] These leading research results suggest that there is a great potential to utilize SHC for

Received: June 21, 2014
Revised: August 19, 2014
Published: August 19, 2014

dx.doi.org/10.1021/ef501386g | *Energy Fuels* 2014, 28, 6140−6150

Table 1. Characteristics of Dewatered Sewage Sludge, Sewage-Sludge-Derived Hydrochars, and Three Different-Rank Coals[a]

	proximate analysis (wt %, db)				ultimate analysis (wt %, db)					calorific analysis (MJ/kg, db)	
sample	ash	VM	FC	fuel ratio[b]	C	H	N	S	O[c]	HHV	LHV[d]
DSS	21.80	69.01	9.19	0.13	39.88	6.20	6.04	5.62	20.46	17.97	16.61
SHC-220	35.82	51.82	12.36	0.24	41.43	5.09	4.48	4.04	9.14	18.52	17.40
SHC-260	37.78	47.06	15.16	0.32	43.92	5.03	3.92	4.04	5.30	19.43	18.32
SHC-300	38.80	18.24	42.96	2.36	44.48	5.03	3.73	3.94	4.03	20.30	19.19
SHC-320	40.11	12.86	47.03	3.66	43.74	4.86	3.56	3.73	4.00	20.35	19.28
SHC-340	41.17	42.03	16.80	0.40	44.38	4.83	3.52	3.68	2.42	20.23	19.17
SHC-380	43.20	38.25	18.55	0.48	42.99	4.46	3.22	3.56	2.57	19.58	18.60
Coal-1	3.36	31.11	65.54	2.11	71.96	4.54	0.76	2.02	17.36	28.85	27.86
Coal-2	17.22	48.95	33.84	0.69	50.34	5.37	0.98	2.98	23.11	22.63	21.45
Coal-3	9.93	32.66	57.41	1.76	62.77	3.66	0.64	2.52	20.48	24.37	23.57

[a]Abbreviations: db, dry basis; VM, volatile matter; FC, fixed carbon; HHV, higher heating value; LHV, lower heating value. [b]Calculated as FC/VM. [c]Calculated by difference on a dry, ash-free basis. [d]Calculated using the formula LHV_{dry} (MJ/kg) = HHV_{dry} (MJ/kg) − 2.4418 × (9 × H_{dry}/100) (MJ/kg).

existing cofiring infrastructures toward lower coal consumption and better management of SS.

Nonetheless, the existence of interactions between different solid fuels during cocombustion could lead to variations in fuel reactivity and burnout characteristics since the cocombustion performance may not necessarily demonstrate synergistic interactions or simple additive behaviors as expected.[11] Thus, extensive research regarding interaction effects during cocombustion has been conducted, including studies of cocombustion of SS and coals[5,12] and cocombustion of biomass or pretreated biomass and coals.[13,14] In particular, Parshetti et al.[7] studied cocombustion of low-rank Indonesian coal and SHC with blending ratios ranging from 10% to 30%. Increasing the amount of SHC improved the combustion reactivity of the blend. In addition, Liu et al.[15] concluded that synergistic interactions between hydrochar and low-rank coals were more intense than those with high-rank coals because of their similar fuel characteristics. However, in order to enhance the combustion reactivity, SHC of better fuel quality is desired. From the perspective of considerable reduction in coal consumption, greater SHC blending ratios in cofiring are more economically viable. To date, limited information and systematic research is available pertaining to the evolution of fuel characteristics and combustion behavior of SHCs derived from different hydrothermal conditions and cocombustion performance with different-rank coals.

Therefore, it is meaningful to screen SHCs of good fuel quality for cocombustion with different coals over a wide range of blending ratios before designing cocombustion scenarios. To fill up this research gap, the main objectives of this study are (1) to investigate fuel characteristics and combustion behaviors of SHCs prepared under various hydrothermal conditions to screen the best SHC for cocombustion; (2) to compare the combustion behaviors of three different-rank coals with SHCs; (3) to analyze the cocombustion behaviors for the selected SHC and three different-rank coals over a wide range of coal/SHC blending ratios; and (4) to interpret interaction effects during the cocombustion process.

2. EXPERIMENTAL SECTION

2.1. Materials. DSS was collected from Ulu Pandan Water Reclamation Plant in Singapore. After the anaerobic digestion and dewatering process, the generated DSS possessed 82.5 wt % water. The DSS sample was stored in a 4 °C cold room and used directly as a feedstock to prepare hydrochar solid fuels using hydrothermal conversion (HTC). Three different-rank coals originating from China, namely, Hongshaquan coal, Shuicheng lignite, and Shaerhu coal (designated as Coal-1, Coal-2, and Coal-3, respectively) were obtained. Prior to characterization, all of the DSS, hydrochar, and coal samples were oven-dried at 105 °C overnight and ground into fine powders (less than 0.5 mm) using a rotary mill. These samples were sealed in dry polypropylene centrifuge tubes and stored in a dry cabinet.

2.2. HTC Experiments. HTC of DSS was conducted in a 1.0 L stainless steel (SS 316L) fixed-head batch reactor (Parr model 4577) equipped with a magnetic drive stirrer, external electric heating mantle, and PID controller (Parr Instrument Co., Moline, IL, USA). The reactor was designed to withstand a maximum operating temperature and pressure of 500 °C and 35 MPa, respectively. The temperature was precisely controlled by a J-type thermocouple. The pressure was autogenously generated by the water in the DSS at the corresponding temperature and was shown on both an analogue gauge and a digital indicator. On the basis of records from preliminary experiments, 150 g of deionized water could generate a pressure of 22.0 MPa at 380 °C, which reached near-critical water conditions. In each batch experiment run, 182 g of DSS, which contained approximately 150 g of water, was loaded into the reactor vessel. Subsequently, the vessel was sealed and then heated to the preset temperature and corresponding pressure using an electric heating mantle under a stirring speed of 500 rpm. Following the above procedure, six sets of HTC conditions were applied: 220 °C and 2.6 MPa, 260 °C and 5.0 MPa, 300 °C and 9.3 MPa, 320 °C and 12.0 MPa, 340 °C and 15.5 MPa, and 380 °C and 22.0 MPa. After a reaction time of 20 min under the desired temperature and pressure, the heating mantle was removed. The vessel was first cooled by a standing fan. When the temperature was below 200 °C, an additional internal cooling coil was then employed to quench the vessel rapidly to room temperature via a cooling water circulator.

After depressurization, the vessel was opened for separation and collection of solid and liquid products. The liquid products were filtered through 0.45 μm PTFE membrane filters and kept in glass vials at 4 °C for further analysis. The solid residues were carefully collected and oven-dried at 105 °C for 12 h. The dry solids were ground into fine powders (less than 0.5 mm) and termed hydrochars hereinafter. The SHCs were designated as SHC-220, SHC-260, SHC-300, SHC-320, SHC-340, and SHC-380, respectively. The number indicates the reaction temperature.

2.3. Characterization of Samples. For proximate analysis, the ash content determinations were carried out according to ASTM D3174 and VM contents were measured using an STA 449 F3 Jupiter simultaneous TG-DTA/DSC apparatus (NETZSCH-Gerätebau GmbH) according to ASTM D7582-10. The fixed carbon (FC) percentage was then calculated by difference. Moreover, the fuel ratio,

dx.doi.org/10.1021/ef501386g | Energy Fuels 2014, 28, 6140−6150

which is expressed as the ratio of FC to VM, represents the fuel properties of solid fuels, and high-rank coals generally exhibit high fuel ratios.[6,16] In this study, the fuel ratio was used to present the evolution of FC and VM during HTC and to reflect the solid fuel quality of derived hydrochars for cofiring applications. The elemental compositions (i.e., carbon, hydrogen, nitrogen, and sulfur) of DSS, hydrochars, and coals were determined using a vario EL CHNS elemental analyzer. The HHVs for all of the solid fuel samples were measured using an IKA C2000 BASIC bomb calorimeter. Table 1 summarizes basic fuel characteristics of DSS, the SHCs, and the three different-rank coals.

2.4. Preparation of Hydrochar and Coal Blends. Because SHC-320 showed the highest HHV (20.35 MJ/kg), greatest fuel ratio (3.66), and relatively low N and S contents, the coal/hydrochar blends were prepared by thoroughly mixing SHC-320 with the three Chinese coals. Different coal/SHC-320 blending ratios (i.e., 30:70, 50:50, and 70:30) were selected. According to these blending ratios, coal and hydrochars were loaded into beakers and well-dispersed in water by magnetic stirring at 650 rpm for 24 h at room temperature. Afterward, the mixtures were oven-dried at 105 °C for 24 h and ground into fine powders for subsequent combustion behavior analysis. In order to easily identify the different coal/hydrochar blends, they are designated as 30C70HC-1, 50C50HC-1, 70C30HC-1, 30C70HC-2, 50C50HC-2, 70C30HC-2, 30C70HC-3, 50C50HC-3, and 70C30HC-3, respectively. In these labels, "C" represents the coal sample and the number before "C" is the blending ratio (%) of coal, while "HC" represents the SHC-320 sample and the number before "HC" is the blending ratio (%) of SHC-320; the number after the hyphen stands for the coal rank (i.e., "1" represents Coal-1, "2" represents Coal-2, and "3" represents Coal-3).

2.5. Analyses of Combustion Characteristics. *2.5.1. Thermogravimetric Analysis (TGA).* In this study, the combustion behaviors of solid fuel samples were analyzed by means of the widely used TGA method using a PerkinElmer TGA7 thermogravimetric analyzer. Combustion experiments were performed according to the procedure described in our previous study.[10] In each run, 9 mg of sample was loaded into the TG pan and heated from 30 to 900 °C at a heating rate of 10 °C/min with a fixed air flow rate of 20 mL/min under atmospheric pressure. The weight loss (TG) and the rate of weight loss (DTG) of each sample under non-isothermal conditions were recorded dynamically and used for evaluation of the combustion performance and kinetics analysis of different solid fuel samples. Repeated combustion runs of samples were conducted to verify the reproducibility of the experimental results and ensure that the deviations were less than 5%.

2.5.2. Kinetics Analysis. In general, the reaction kinetics during the combustion process can be expressed according to the decomposition rate of solid fuels as described previously:[10,15]

$$\frac{d\alpha}{dt} = kf(\alpha) \tag{1}$$

$$\alpha = \frac{m_i - m}{m_i - m_f} \tag{2}$$

$$f(\alpha) = (1-\alpha)^n \tag{3}$$

$$k = A\exp\left(-\frac{E}{RT}\right) \tag{4}$$

$$\beta = \frac{dT}{dt} \tag{5}$$

where α is the thermal conversion fraction of the solid fuel at time t; m_i, m, and m_f refer to the initial, instantaneous, and final mass of the solid fuel, respectively; $f(\alpha)$ represents a general expression for the combustion mechanism; n is the order of the reaction; k is the rate constant, which can be derived from the Arrhenius equation (eq 4), in which E and A represent the activation energy (kJ mol^{-1}) and the pre-exponential factor (min^{-1}) of the reaction, respectively; R is the universal gas constant (8.314 J K^{-1} mol^{-1}); T is the absolute temperature (K); and β denotes a constant heating rate (10 °C/min) in the present non-isothermal combustion study.

A series of combinations and rearrangements of eqs 1 − 5 gives

$$\frac{d\alpha}{f(\alpha)} = A\exp\left(-\frac{E}{RT}\right)dt = \frac{A}{\beta}\exp\left(-\frac{E}{RT}\right)dT \tag{6}$$

Integration of eq 6 gives

$$G(\alpha) = \int_0^\alpha \frac{d\alpha}{f(\alpha)} = \int_{T_0}^{T} \frac{A}{\beta}\exp\left(-\frac{E}{RT}\right)dT \tag{7}$$

Transformation of eq 7 based on the Coats−Redfern approximation method[17] for analysis of the kinetic parameters in the non-isothermal combustion process[14] gives

$$\ln\left[\frac{G(\alpha)}{T^2}\right] = \ln\frac{AR}{\beta E}\left(1 - \frac{2RT}{E}\right) - \frac{E}{RT} \tag{8}$$

Since $RT/E \ll 1$ and thus $1 - RT/E \approx 1$ in this study, the kinetic mechanism equation for the combustion process can be described as shown in eq 9:[10]

$$\ln\left[\frac{G(\alpha)}{T^2}\right] = \ln\frac{AR}{\beta E} - \frac{E}{RT} \tag{9}$$

When an appropriate value of n is selected, a straight line can be obtained by plotting $\ln[G(\alpha)/T^2]$ versus $1/T$. Hence, E and A can be determined from the slope and intercept of this line, respectively.

2.5.3. Evaluation of Combustion Performance. Three characteristic temperatures, namely, the ignition temperature (T_i, °C), the maximum combustion rate temperature (T_m, °C), and the burnout temperature (T_b, °C), were derived from the TG-DTG data. Three points (i.e., points A, B, and C in all of the figures) were identified following a previously described procedure.[10,15,18]

According to the characteristic temperatures and representative weight loss rates in combustion profiles, a comprehensive combustibility index (S) was calculated to evaluate the overall combustion reactivity of the solid fuels:[10]

$$S = \frac{(dw/dt)_{max}(dw/dt)_{mean}}{T_i^2 T_b} \tag{10}$$

where $(dw/dt)_{max}$ and $(dw/dt)_{mean}$ are the maximum and mean rates of weight loss (wt %/min), respectively.

2.5.4. Deviation between Experimental and Theoretical Combustion Profiles. To investigate interaction phenomena of hydrochars and coals during their cocombustion, theoretical TG and DTG curves were calculated by taking account of the individual mass fraction, weight loss, and rate of weight loss of SHC-320 and the coals as follows:[19,20]

$$(TG)_{cal} = x_1(TG)_{hydrochar} + x_2(TG)_{coal} \tag{11}$$

$$\left(\frac{dw}{dt}\right)_{cal} = x_1\left(\frac{dw}{dt}\right)_{hydrochar} + x_2\left(\frac{dw}{dt}\right)_{coal} \tag{12}$$

where $(TG)_{hydrochar}$ and $(TG)_{coal}$ are normalized weight losses derived from TG curves for independent combustion of SHC-320 and the coal, respectively; $(dw/dt)_{hydrochar}$ and $(dw/dt)_{coal}$ are normalized rates of weight loss derived from DTG curves for independent combustion of SHC-320 and the coal, respectively; and x_1 and x_2 are the mass fractions of SHC-320 and the coal in the blend, respectively.

Deviations between the maximum weight loss rates and residues for the experimental and calculated curves can be used to quantify whether synergistic interactions occurred after addition of hydrochars to the coals. The deviations were determined according to eq 13:

$$\text{deviation} = \frac{\text{exp value} - \text{cal value}}{\text{cal value}} \times 100\% \tag{13}$$

dx.doi.org/10.1021/ef501386g | Energy Fuels 2014, 28, 6140−6150

3. RESULTS AND DISCUSSION

3.1. Physicochemical Properties of DSS, Hydrochars, and Coals. *3.1.1. Effects of HTC on Fuel Characteristics of Hydrochars.* As shown in Table 1, DSS consisted of 69.01% VM, 9.19% FC, and 21.80% ash, leading to a low fuel ratio (FC/VM) of 0.13. The high N and S contents (6.04% and 5.62%, respectively) imply significant pollutant emissions when DSS is directly utilized as a solid fuel. The high S content may originate from enriched alkyl surfactant and perfluorooctanesulfonate compounds in DSS. The high O content (20.46%) could be detrimental to the calorific value of DSS. Consequently, the HHV and lower heating value (LHV) of DSS were 17.97 and 16.61 MJ/kg, respectively.

The VM content of DSS decreased significantly after HTC: DSS had a VM content of 69.01%, which decreased to 12.86% in SHC-320 with the increased temperature and pressure. The lost VM was converted into FC and gaseous products via dehydration and decarboxylation reactions,[10] and thus, the FC of hydrochars increased progressively from 9.19% in DSS to 47.03% in SHC-320. As a result of increased generation and deposition of light volatile organic molecules on the surface of the hydrochars,[10,21] the VM contents of hydrochars produced by severe hydrothermal treatment (i.e., 340 °C and 15.5 MPa or 380 °C and 22.0 MPa) were at least 3 times higher than that of SHC-320. However, further degradation and transformation of these volatile molecules in hydrochars tended to be obvious under even higher temperature and pressure. Compared with SHC-340, the VM content decreased from 42.03% to 38.25% in SHC-380, while the slight increase (1.75%) in FC in SHC-380 may be associated with partial conversion of the VM. Furthermore, the excess loss of VM and retained minerals resulted in a constant increase in ash content (ca. 40%) in hydrochars under all of the HTC conditions. Accordingly, the fuel ratio increased from 0.13 for DSS to 3.66 for SHC-320 and decreased to around 0.40 afterward.

On the basis of ultimate analysis results, the H, N, S, and O contents in the hydrochar declined as the temperature and pressure increased. In particular, within a reaction time of 20 min at 380 °C and 22.0 MPa, the efficiency of N, S, and O removal reached 47%, 37%, and 87.4%, respectively. On the other hand, the C content increased to around 43% to various extents. As a result of the remarkable removal of O and the increase in C content, the calorific values of the hydrochars were increased by 1.03 to 1.13 times. When the evolutions of the three components (i.e., ash, VM, and FC) and the elemental compositions in hydrochars are taken into account, SHC-320 exhibited the highest HHV and LHV (20.35 and 19.28 MJ/kg, respectively). Hence, from the perspectives of superior fuel characteristics compared with DSS and the other hydrochars, SHC-320 was selected as the sewage-sludge-derived solid fuel for cocombustion with coals.

3.1.2. Fuel Characteristics of Different-Rank Coals. The coal samples showed great differences in components and elemental compositions compared with DSS and the hydrochars. As shown in Table 1, the FC contents in the coals were 3.68 to 7.13 times higher than that in DSS, whereas the VM contents were generally lower than the value of 69.01% in DSS. Coal-1 and Coal-2 presented the highest contents of FC (65.54%) and VM (48.95%), respectively. The fuel ratios of the three different-rank coals were 2.11, 0.69, and 1.76 for Coal-1, Coal-2, and Coal-3, respectively. The ash contents in the coals were typically lower than 20%, and Coal-1 contained only 3.36% ash. The C contents (50.34−71.96%) in the coals were much higher than the value of 39.88% in DSS, while the H, N, and S contents were relatively lower. Especially, the N and S contents in all of the coal samples were less than 1% and 3%, respectively. In addition, the O content was around 20%, which is comparable to that in DSS but much higher than those in the hydrochars. Because of the higher C contents but lower ash contents, the HHVs of the coals (28.85, 22.63, and 24.37 MJ/kg for Coal-1, Coal-2, and Coal-3, respectively) were higher than the value of 17.97 MJ/kg for DSS. Overall, the coal rank followed the order Coal-1 > Coal-3 > Coal-2 in terms of these fuel characteristics.

3.2. Effects of HTC on Combustion Profiles and Characteristics of Hydrochars. To investigate the combustion behaviors of DSS and the hydrochars, the entire decomposition profiles were characterized according to evident rates of weight loss in DTG curves. As described by He et al.,[10] the combustion process generally consisted of a dehydration stage (D), a devolatilization and combustion stage (E), a char combustion stage (F), and a burnout stage.

Previously, a two-stage decomposition kinetics model was proposed to assess the combustion of biomass.[14,22] However, to take into account the delayed combustion of heavy VM and FC in solid fuels, a modified two-stage combustion scheme was employed in the present study to describe the combustion process, as follows:

first combustion stage (E_1, A_1):

$$V_1(\text{light volatile matter}) \rightarrow C_1(\text{char}) + G_1(\text{gas})$$

second combustion stage (E_2, A_2):

$$V_2(\text{heavy volatile matter}) + C_1(\text{char}) + C_2(\text{fixed carbon}) \rightarrow G_2(\text{gas}) + R(\text{ash})$$

where E_1 and A_1 represent the activation energy and pre-exponential factor, respectively in the first combustion stage and E_2 and A_2 represent the activation energy and pre-exponential factor, respectively, in the second combustion stage.

Subsequently, kinetics analyses of individual combustion stages were performed separately using the Arrhenius equation by selecting an appropriate reaction order.

3.2.1. Combustion of DSS. As shown in Figure 1, stage D (30 to 100 °C) was the initial water evaporation stage, and two

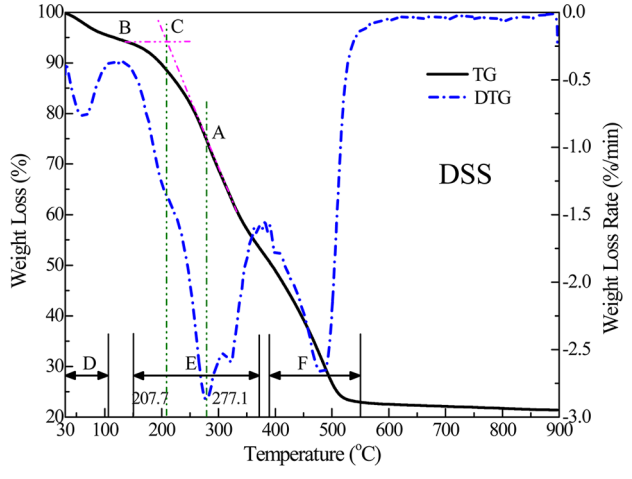

Figure 1. TG and DTG curves for combustion of DSS.

dx.doi.org/10.1021/ef501386g | Energy Fuels 2014, 28, 6140−6150

Table 2. Combustion Stages, Weight Losses during the Main Combustion Stages, Characteristic Temperatures, Total Burnout Times, and Residues after Combustion

	temperature ranges (°C)			weight loss (%)			characteristic temperatures (°C)			
sample	stage D	stage E	stage F	stage E	stage F	residues (%)	T_i	T_m	T_b	t_b[a] (min)
DSS	~100	150−370	390−550	39.9	27.7	21.4	207.7	278.8	514.9	30.7
SHC-220	~100	200−350	350−550	22.5	37.0	34.2	277.1	431.2	506.9	23.0
SHC-260	~100		200−550		57.6	36.8	301.4	428.3	501.1	20.0
SHC-300	~100	150−260	270−550	6.6	49.2	39.6	301.4	405.4	507.9	20.7
SHC-320	~100	150−260	300−550	7.7	46.4	38.4	301.4	413.5	506.0	20.5
SHC-340	~100	150−270	300−550	8.7	46.0	39.3	312.6	426.3	517.8	20.5
SHC-380	~100	150−270	300−550	8.9	40.9	42.9	315.9	417.9	557.7	24.2
Coal-1	~100		410−550		75.2	2.7	409.8	473.0	543.3	13.4
30C70HC-1	~100	205−280	350−550	4.1	47.8	28.2	348.2	439.0	597.5	24.9
50C50HC-1	~100	200−280	410−550	3.1	47.7	20.5	406.4	526.3	593.9	18.8
70C30HC-1	~100		410−550		58.8	12.9	429.1	518.9	587.1	15.8
Coal-2	~100		290−520		68.5	14.6	288.4	373.1	487.3	19.9
30C70HC-2	~100	200−270	300−520	4.5	51.2	32.6	299.7	401.6	535.8	23.6
50C50HC-2	~100	220−300	300−520	4.7	54.9	26.6	298.2	352.4	538.7	24.1
70C30HC-2	~100		250−520		64.9	23.1	309.5	346.6	526.3	21.7
Coal-3	~100		350−520		71.6	5.7	367.6	403.8	501.0	13.3
30C70HC-3	~100	200−270	340−550	4.5	50.8	29.2	345.0	421.1	539.5	19.5
50C50HC-3	~100	200−270	340−550	3.0	56.8	22.8	374.2	429.6	546.9	17.3
70C30HC-3	~100		370−520		57.3	15.1	375.7	427.3	518.6	14.3

[a] t_b is the burnout time, which runs from the time corresponding to T_i until the time corresponding to T_b.

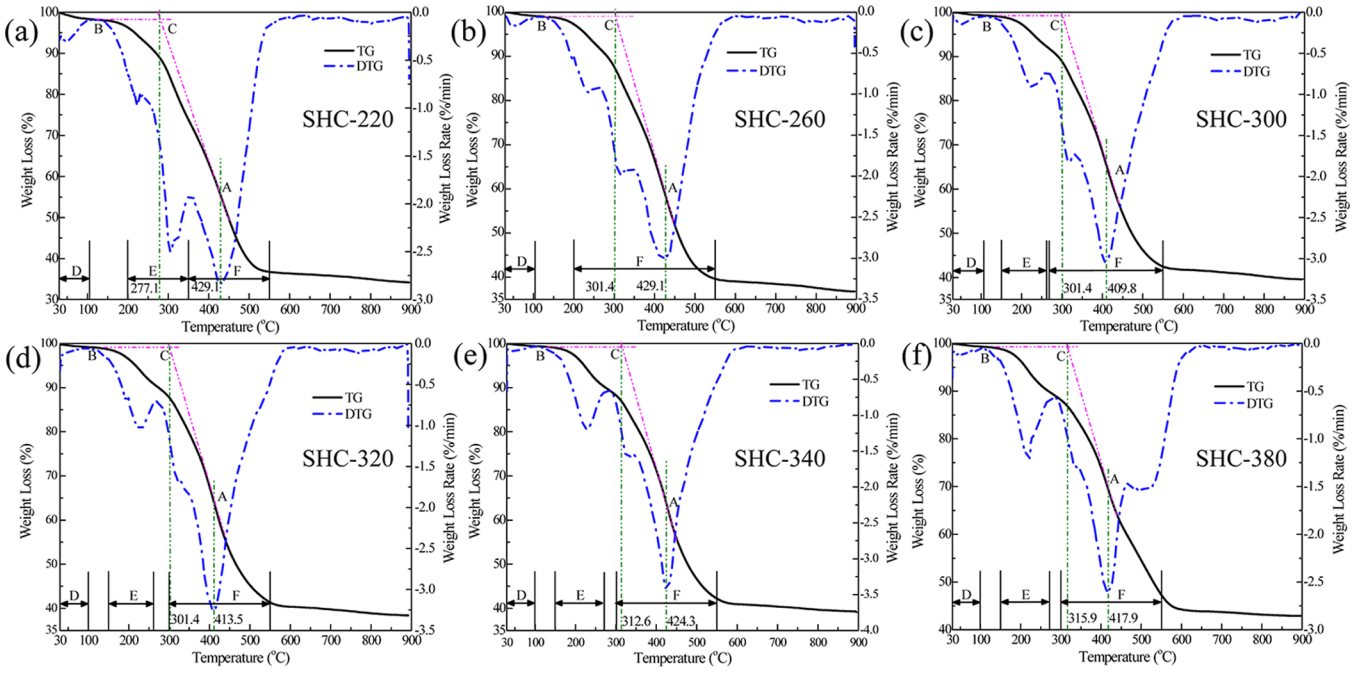

Figure 2. TG and DTG curves for combustion of hydrochars derived at different temperatures and pressures.

distinct decomposition stages (E and F) governed the intense combustion process of DSS. Unlike the single combustion profile (250 to 450 °C) of DSS in our previous study,[10] the two-stage combustion profile was associated with the noticeable FC content (9.19%) of DSS in this study. As summarized in Table 2, the first combustion stage (E) was extended from 150 to 370 °C while the second combustion stage (F) was from 390 to 550 °C, which was similar to the main combustion process of microalgae under comparable conditions as reported by Tahmasebi et al.[23] Two pronounced peaks were observed at 277.1 and 483.7 °C. The peak temperatures at 277.1 and 320.5 °C during stage E may be related to the stepwise decomposition of carbohydrates (180−270 °C) and proteins and lipids (320−450 °C),[23−25] while the peak temperature around 483.7 °C in stage F could be ascribed to residual lignin decomposition and char/FC oxidation.[26,27] Moreover, the weight loss in stage E (39.9%) was higher than that in stage F (27.7%), suggesting more light VM in DSS. T_i is associated with the rate of release of heat from early combustion of light VM.[26] As a result, T_i was only 207.7 °C and the maximum weight loss was at 278.8 °C, which were quite close. However, the high T_b (514.9 °C) led to a prolonged combustion process

dx.doi.org/10.1021/ef501386g | Energy Fuels 2014, 28, 6140−6150

Table 3. Combustion Kinetic Parameters for DSS, the Hydrochars, the Three Different-Rank Coals, and Their Respective Blends with SHC-320

sample	temperature range (°C)	E (kJ mol^{-1})	A (min^{-1})	n	R^2
DSS	150−370	18.12	1.43	1	0.9873
	390−550	32.31	26.14	1	0.9501
SHC-220	200−350	26.43	6.59	1	0.9911
	350−550	32.29	23.58	1	0.9883
SHC-260	200−550	29.97	13.86	1	0.9942
SHC-300	150−260	30.53	18.11	1	0.9920
	270−550	32.13	20.58	1	0.9952
SHC-320	150−260	28.98	14.50	1	0.9957
	300−550	32.60	22.70	1	0.9927
SHC-340	150−270	34.49	59.59	1	0.9899
	300−550	33.60	25.68	1	0.9894
SHC-380	150−270	31.62	33.86	1	0.9821
	300−550	27.61	6.60	1	0.9910
Coal-1	410−550	87.60	2.22×10^{05}	1	0.9953
30C70HC-1	205−280	13.66	0.10	1	0.9973
	350−550	37.69	25.80	1	0.9911
50C50HC-1	200−280	8.84	0.02	1	0.9923
	410−550	50.03	205.24	1	0.9809
70C30HC-1	410−550	61.74	1653.08	1	0.9798
Coal-2	290−520	39.07	101.81	1	0.9919
30C70HC-2	200−270	42.82	218.33	1	0.9942
	300−520	38.69	61.21	1	0.9962
50C50HC-2	220−300	13.20	0.10	1	0.9964
	300−520	38.06	52.44	1	0.9963
70C30HC-2	250−520	45.84	222.23	1	0.9796
Coal-3	350−520	62.22	5092.79	1	0.9893
30C70HC-3	200−270	12.97	0.14	1	0.9900
	340−550	40.11	72.19	1	0.9923
50C50HC-3	200−270	4.35	0.01	1	0.9915
	340−550	44.37	140.07	1	0.9860
70C30HC-3	370−520	58.35	2115.05	1	0.9909

of 30.7 min. The water evolution and releases of small amounts of methane and carbon dioxide could be responsible for the first peak, whereas intensive decompositions of aromatic or heterocyclic hydrocarbons led to significant emissions of hydrogen, methane, and carbon dioxide in the second peak due to the abundant VM and O contents.[24,25] Nevertheless, further investigations are necessary to gain more insight into the gas evolutions.

3.2.2. Combustion of Hydrochars. Figure 2 illustrates combustion profiles of different hydrochars. Dehydration of the hydrochars (stage D) was less obvious with increases in temperature and pressure, which should be relevant to the more hydrophobic characteristics of hydrochars.[10] Besides, the peak in stage E became less intense while that in stage F tended to be sharper. The weight loss in stage E decreased to 22.5% for SHC-220, but that in stage F increased to 37.0%. The combustion kinetics of SHC-260 (Table 3) indicated that there may be an overlap of stages E and F, causing a broad stage F (200−550 °C) with a great mass loss of 57.6%. As shown in Table 2, the weight loss in stage F decreased from 49.2% for SHC-300 to 40.9% for SHC-380 as a result of accelerated depolymerization and repolymerization of heavy VM in subcritical water.[28] On the other hand, during HTC of sludge, formation of water-soluble oil was favored at lower temperatures while increased temperature led to higher yields of water-insoluble heavy oil (HO).[29] HO was mainly composed of long-chain carboxylic acids, phenolic compounds, and derivatives. Since the hydrochars in this study were not extracted with solvent, HO could be entrained. These small amounts of light volatile compounds contributed to a slight increase in weight loss in stage E from 6.6% for SHC-300 to 8.9% for SHC-380. One apparent peak was observed at around 200 °C. An increasing trend of residues agreed with previous discussion.

Because of the reduced VM content and elevated FC content in the hydrochars, T_i exhibited a remarkable increase of 70 to 108 °C as the temperature and pressure increased. Low T_i may cause a potential fire hazard.[15,30] In this regard, hydrochars demonstrated advantages in safe handling and storage over DSS. Though the VM contents in SHC-340 and SHC-380 were much higher than the lowest VM in SHC-320, the T_i values of the former hydrochars were even higher, suggesting that a high VM does not necessarily give a lower T_i. Further, T_m also increased drastically to different extents to around 420 °C for hydrochars. There was a minor decrease in T_b within 10 °C for hydrochars derived at HTC temperatures lower than 320 °C. On the contrary, T_b increased to 517.8 and 557.7 °C for SHC-340 and SHC-380, respectively. The noticeable decrease in FC content and the relatively high ash content should be responsible for the difficult combustion. In particular, an evident shoulder in stage F for SHC-380 appeared at high temperature (470−550 °C). Main combustion was shortened to approximately 20 min, but combustion of SHC-380 lasted 24.2 min, which was the highest among the SHCs. Therefore, in terms of safer T_i, higher heat release in a higher temperature

dx.doi.org/10.1021/ef501386g | Energy Fuels 2014, 28, 6140−6150

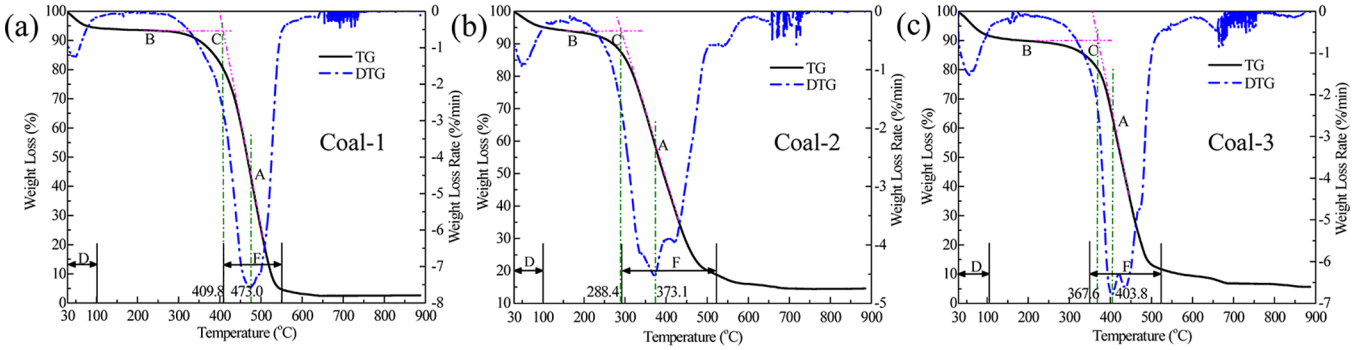

Figure 3. TG and DTG curves for combustion of the three different-rank coals.

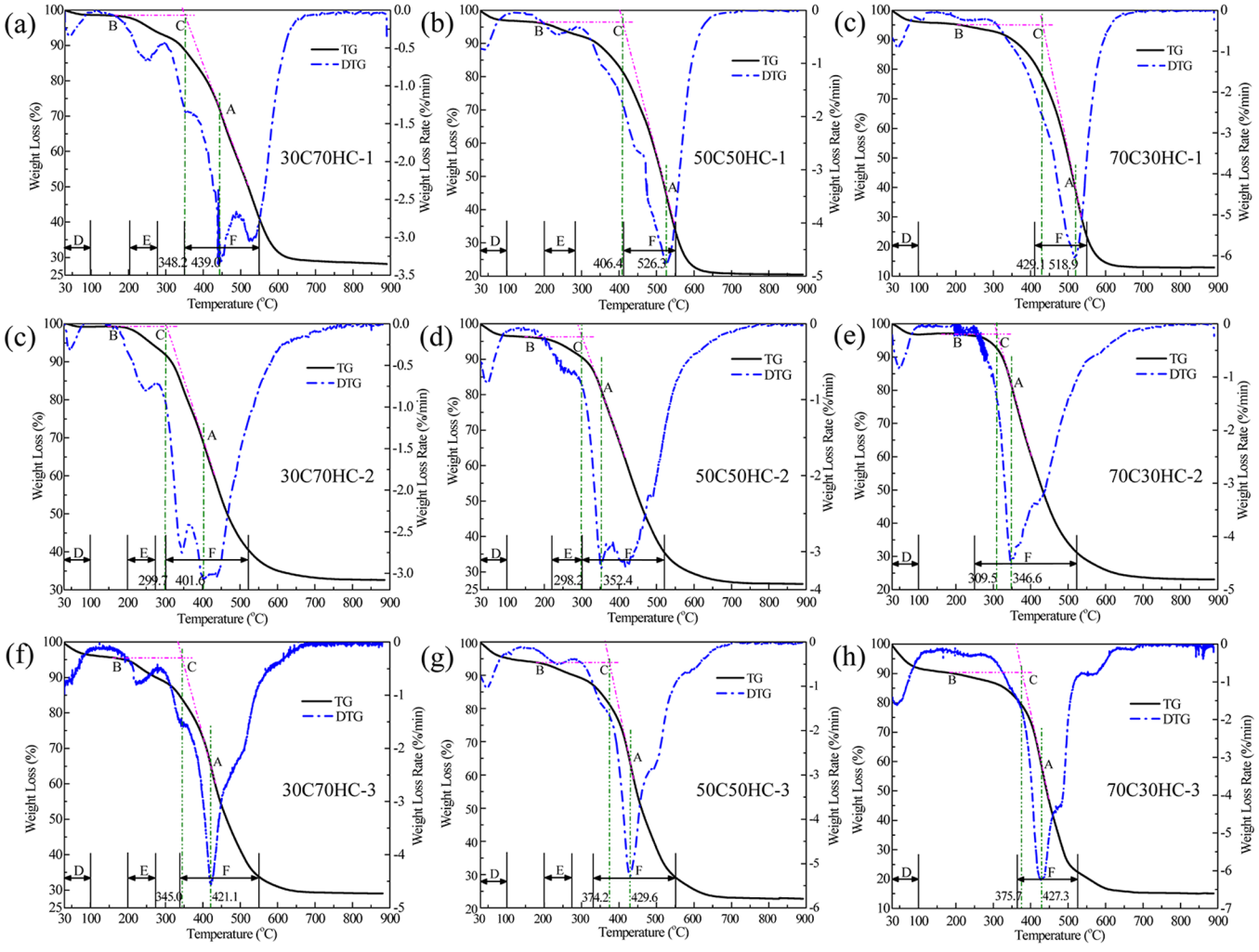

Figure 4. Cocombustion profiles for blends of SHC-320 with different-rank coals at three blending ratios.

region, and slightly decreased T_b during the shortened combustion profile, the performance of SHC-320 outweighed that of the other SHCs.

3.3. Combustion Profiles for Different-Rank Coals. As shown in Figure 3, main combustion of coals was characterized by only stage F. This suggests that decomposition of VM during coal combustion requires a higher temperature as FC, resulting in remarkable weight loss and simultaneous oxidation of heavy VM and FC[23,31] within a narrow stage F at high temperatures. Furthermore, higher-rank coal exhibited a narrower stage F and greater weight loss or heat release. In Table 2, the width of the temperature range followed the order Coal-1 (410−550 °C) < Coal-3 (350−520 °C) < Coal-2 (290−520 °C) while the weight losses were ordered as Coal-1 (75.2%) > Coal-3 (71.6%) > Coal-2 (68.5%). Overall, T_i, T_m, and T_b increased as the coal rank became higher. The relatively low rank Coal-2 showed T_i and T_m of 288.4 and 373.1 °C, respectively, which were more comparable to those of SHC-320. Typically, t_b was lower for the coals than for DSS and the hydrochars. Interestingly, the t_b values for SHC-320 (20.5 min) and lower-rank Coal-2 (19.9 min) were similar. Thus, a more compatible cocombustion of the two fuels was anticipated.

dx.doi.org/10.1021/ef501386g | Energy Fuels 2014, 28, 6140−6150

Compared with DSS and the hydrochars, the burnout stages of the three coals presented some fluctuations, especially for Coal-2, which produced the highest residues (14.6%) as a result of decomposition of inorganic salts or metal carbonates therein at 550 to 750 °C.

3.4. Effects of Hydrochar on Cocombustion with Different-Rank Coals. *3.4.1. Effects of Coal/Hydrochar Blending Ratio and Different Characteristics of Coals. 3.4.1.1. Patterns of Combustion Profiles.* According to the cocombustion profiles in Figure 4 and the combustion kinetics data in Table 3, lower supplements of coal (30% and 50%) resulted in two-stage combustion (stages E and F), while there was only one distinct stage F at the high coal/SHC-320 ratio (70:30). Nonetheless, the weight loss in stage E was less than 5%. Except for Coal-2, this mass loss was inclined to be slightly lower when the coal/SHC-320 ratio was elevated to 50:50. In contrast, the weight loss in stage F showed an upward trend as the coal/SHC-320 blending ratio varied from 30:70 to 70:30. In addition, compared with the weight loss in stage F for the individual coal, this value for coal/SHC-320-blended fuels declined drastically as the coal rank increased. Specifically, the Coal-2/SHC-320 retained 74.7 to 94.7% of the weight loss value in lower-rank Coal-2, which was higher than the retention by Coal-3/SHC-320 (70.9 to 80.0%) and Coal-1/SHC-320 (63.5 to 78.2%). This reveals that heat loss may be larger during cocombustion of SHC-320 with higher-rank coals. Stage F in the DTG curves for the different coal-blended fuels in Figure 4 was closely examined. In Figure 4a,d,e, in addition to the peak at T_m, there was at least one more subpeak in stage F when low coal percentages of 30% and 50% were employed. This phenomenon may be attributed to less significant synergistic effects resulting from either apparently different or similar characteristics of the two individual fuels. Since the proportion of coal was less, the combustion of coal could not affect that of the hydrochar too much. Meanwhile, though hydrochar made up the majority in blends, it may be inadequate to alter the combustion patterns of coals. Thus, the components in blends of Coal-1 or Coal-2 with SHC-320 may be combusted independently.[7] Some combustibles may overlap, thereby exhibiting several subpeaks in DTG curves. For the rest, especially in Coal-3/SHC-320 blends, the VM and FC components may interact with each other, promoting a combined and short stage F. However, Coal-3/SHC-320 at all blending ratios showed only one sharp peak in stage F, which may be associated with intense synergistic effects. In spite of this, there was a small shoulder at high temperatures. Besides, residues increased to approximately 30% when the coal/SHC-320 blending ratio decreased to 30:70.

3.4.1.2. Evolutions of Characteristic Temperatures. Generally, T_i increased with the coal blending ratio. For the low coal/SHC-320 blending ratio (30:70), the T_i values were 348.2, 299.7, and 345.0 °C for 30C70HC-1, 30C70HC-2, 30C70HC-3, respectively, which fell between the T_i values of SHC-320 and the individual coals. Because T_i for Coal-2 was lower than that for SHC-320 and SHC-320 dominated the blends, T_i for 30C70HC-2 was higher than that for lower-rank Coal-2. Meanwhile, the T_i values for the other two blended fuels were lower compared with their respective coals because of their inherent relatively high T_i (>350 °C). On the other hand, a high blending ratio resulted in a higher T_i for their blends. Hence, in blends of SHC-320 with higher-rank coals, the ignition performance could be improved in the presence of a high proportion of SHC-320 but inhibited when a smaller amount (≤30%) of SHC-320 was introduced.

With an increase in the coal/hydrochar blending ratio, T_m of the blended fuels shifted to lower temperature (ca. 350 °C) for lower-rank Coal-2 because of the higher VM content therein but was at a higher temperature for higher-rank Coal-1 (ca. 520 °C) and Coal-3 (ca. 425 °C). Interestingly, after the introduction of 70% SHC-320, T_m displayed opposite evolutions, decreasing to 439 °C for 30C70HC-1 but increasing to 401.6 °C for 30C70HC-2. This was mainly related to the predominant role of SHC-320 in the blends, resulting in a T_m close to that of SHC-320. Because of the prominent intrinsic characteristics of the two coals, their blends exhibited opposite behaviors.

T_b for all of the blends increased dramatically by ca. 20 to 50 °C to different extents, thereby extending t_b to 24.9 min for 30C70HC-1. Although Coal-2 and SHC-320 presented similar t_b values, the t_b values of their blends were obviously greater. It is worth noting that for the same blending ratio, t_b for combustion of SHC-320 with high-rank Coal-1 and low-rank Coal-2 was longer than that of moderate-rank Coal-2. Thus, a shorter combustion process may be expected for blends of SHC-320 with moderate-rank coals.

3.4.2. Analysis and Comparison of Kinetic Parameters. Two important kinetic parameters, the activation energy E and the pre-exponential factor A, were determined to obtain in-depth insights into the combustion behaviors of DSS, the hydrochars, the coals, and their respective blends. On the basis of the two-stage combustion scheme proposed in section 3.2 and the different combustion stages in the TG-DTG curves, data derived from individual stages were carefully screened and applied for kinetics analysis through linear regression by selecting the most suitable reaction order. As shown in Table 3, the first-order oxidative mechanism was the best-fitting and most reliable model, with correlation coefficient (R^2) ranging from 0.9501 to 0.9973, in agreement with claims from combustions of DSS, hydrochars, and hydrochar/lignite blends.[7,10,15,27] Moreover, the kinetic parameters derived from the TG-DTG curves with a constant heating rate and the isoconversional method were in good agreement in qualitative terms.[32] Thus, the kinetics data were interpreted for comparison below.

DSS showed lower E_1 and A_1 (18.12 kJ mol^{-1} and 1.43 min^{-1}, respectively) for the first combustion stage but higher E_2 and A_2 (32.31 kJ mol^{-1} and 26.14 min^{-1}, respectively) for the second combustion stage. After HTC, E_1 for the hydrochars increased by 8.31−16.37 kJ mol^{-1} to around 30 kJ mol^{-1}, confirming the better reactivity of DSS compared with the hydrochars at low temperatures. In particular, the E_1 values for SHC-220 and SHC-320 were relatively lower (26.43 and 28.98 kJ mol^{-1}, respectively) while E_1 for SHC-340 was the highest (34.49 kJ mol^{-1}), which was in relation to their T_i values. This indicates that SHC-220 and SHC-320 may be more reactive to ignite than the other hydrochars. Interestingly, excluding SHC-380, the E_2 values for all of the other hydrochars were similar to that of DSS, suggesting comparable energies to oxidize char and FC. Compared with DSS, A_1 for the hydrochars increased while A_2 decreased slightly as a result of compensation effects. SHC-380 had the lowest E_2 (27.61 kJ mol^{-1}) and A_2 (6.60 min^{-1}), which could be mainly attributed to the lower concentrations of heavy VM and FC therein, as A is closely related to the concentrations of reactants on the basis of collision theory.[33]

dx.doi.org/10.1021/ef501386g | Energy Fuels 2014, 28, 6140−6150

Higher-rank coal presented greater activation energy and pre-exponential factor, which followed the order Coal-1 (87.60 kJ mol^{-1} and 2.22 × 10^5 min^{-1}) > Coal-3 (62.22 kJ mol^{-1} and 5092.79 min^{-1}) > Coal-2 (39.07 kJ mol^{-1} and 101.81 min^{-1}). However, the E values for coal blends in all combustion stages were lower than those of their respective coals. E_1 decreased with elevated percentages of coals, suggesting a decrease in the energy needed to initiate decomposition of coal-blended fuels.[33] On the other hand, E_2 gradually increased as the percentage of coal in the blend increased from 30% to 70% (37.69 to 61.74 kJ mol^{-1} for Coal-1/SHC-320; 38.69 to 45.84 kJ mol^{-1} for Coal-2/SHC-320; 40.11 to 58.35 kJ mol^{-1} for Coal-3/SHC-320), pointing out that higher energy is required to overcome barriers resulting from ring-opening, depolymerization, recondensation, and repolymerization reactions.[34] A similar trend was observed for the A values: as the percentage of coal was elevated to 70%, A_2 increased drastically to 1653.08, 222.23, and 2114.05 min^{-1} for 70C30HC-1, 70C30HC-2, and 70C30HC-3, respectively, whereas A_1 approached zero.

3.4.3. Evaluation of Combustion Performance. Table 4 presents $(dw/dt)_{mean}$, $(dw/dt)_{max}$, and S values for DSS, the hydrochars, the coals, and the coal/SHC-320 blends. DSS exhibited the greatest S (11.63 × 10^{-8}) among all of the solid fuels, including the three coals. This was primarily contributed by the lowest T_i, as $(dw/dt)_{mean}$ (0.90 wt %/min) and $(dw/dt)_{max}$ (2.87 wt %/min) for DSS were far lower than $(dw/dt)_{mean}$ (1.12 wt %/min) and $(dw/dt)_{max}$ (7.58 wt %/min) for highest-rank Coal-1. Since low T_i (<220 °C) could pose a fire hazard, especially during co-milling of DSS and coals, it is not advisible to directly utilize DSS as a solid fuel. SHC-220 and SHC-320 presented higher S values around 5 × 10^{-8} among the hydrochars. Similarly, despite relatively lower $(dw/dt)_{mean}$ (0.98 wt %/min) and $(dw/dt)_{max}$ (4.54 wt %/min), lower-rank Coal-2 possessed a higher S (10.98 × 10^{-8}) than Coal-1 (9.30 × 10^{-8}) and Coal-3 (10.85 × 10^{-8}). With increasing coal blending percentage, $(dw/dt)_{mean}$, $(dw/dt)_{max}$, and S increased. Unexpectedly, 70C30HC-3 showed higher $(dw/dt)_{max}$ than 70C30HC-1, although this value for Coal-3 was much lower than that for Coal-1, suggesting that more intense synergistic effects may occur during main combustion. Overall, higher coal percentages of 50% and 70% provided higher S values, and blends of SHC-320 with moderate-rank Coal-3 gave the highest S values compared with the other blends.

Table 4. Comprehensive Combustibility Index Values for DSS, the Hydrochars, the Three Different-Rank Coals, and Their Respective Blends with SHC-320

sample	$(dw/dt)_{mean}$	$(dw/dt)_{max}$	$10^8 \cdot S$
DSS	0.90	2.87	11.63
SHC-220	0.76	2.83	5.53
SHC-260	0.73	2.99	4.79
SHC-300	0.69	3.04	4.55
SHC-320	0.71	3.26	5.04
SHC-340	0.70	3.44	4.76
SHC-380	0.66	2.61	3.10
Coal-1	1.12	7.58	9.30
30C70HC-1	0.82	3.40	3.85
50C50HC-1	0.91	4.79	4.44
70C30HC-1	1.00	6.07	5.62
Coal-2	0.98	4.54	10.98
30C70HC-2	0.77	3.07	4.91
50C50HC-2	0.84	3.22	5.65
70C30HC-2	0.88	4.50	7.85
Coal-3	1.08	6.80	10.85
30C70HC-3	0.81	4.53	5.71
50C50HC-3	0.89	5.29	6.15
70C30HC-3	0.97	6.24	8.27

3.5. Interactions between Hydrochar and Coals during Their Cocombustion. Figure 5 depicts comparisons of the experimental and calculated TG and DTG curves for cocombustion of SHC-320 and different-rank coals. The experimental curves always deviate from the corresponding calculated curves. Compared with the calculated DTG curves, T_m in the experimental DTG curves shifted to higher temperatures for SHC-320 blended with higher-rank Coal-1 and Coal-3 but moved toward lower temperatures for blends with lower-rank Coal-2. In addition, through careful examination of the TG-DTG curves in Figure 5, more remarkable interactions were observed at high temperatures than in the low-temperature region, which coincided with previous findings.[20] In Table 5, the corresponding characteristic parameters at high temperatures, such as T_m, $(dw/dt)_{max}$, and residue contents, obtained from the experimental and calculated TG-DTG curves are shown. Moreover, the deviations between the experimental and calculated data were determined for quantitative comparisons.

The results in Table 5 suggest that both positive and negative interactions between different coals and hydrochars took place during cocombustion. Briefly, a positive $(dw/dt)_{max}$ deviation implies that higher $(dw/dt)_{max}$ can be expected and thus that heat loss could be less, while a positive residue deviation reveals that there are greater combustion difficulties and thus that more incomplete combustion occurs during cocombustion. In this regard, positive $(dw/dt)_{max}$ and negative residue deviations present the most favorable synergistic effects, which is desired during cocombustion of coal/hydrochar blends. Conversely, negative $(dw/dt)_{max}$ and positive residue deviations indicate the highest antisynergistic effects, which should be avoided when designing cocombustion scenarios. Synergistic effect index values were defined and marked accordingly.

On the whole, the deviations for $(dw/dt)_{max}$ varied significantly, while those for residues were within ±7%. 50C50HC-1, 70C30HC-1, and 70C30HC-3 presented the most intense synergistic effects, while 30C70HC-1, 30C70HC-2, and 50C50HC-2 showed the highest antisynergistic effects. Compared with the calculated values, the experimental $(dw/dt)_{max}$ for 30C70HC-2 decreased dramatically by 10.5% with an increase of 4.2% in residues, indicating that a high hydrochar blending ratio (70%) with low-rank coal inhibits cocombustion. Despite the obvious enhancement in $(dw/dt)_{max}$ for 70C30HC-2, 30C70HC-3, and 50C50HC-3, incomplete cocombustion may lead to more residues. Among these three blends, 70C30HC-2 was the most apparent one, demonstrating +17.5% $(dw/dt)_{max}$ and +6.5% residue deviations. It is noted that the higher synergistic effect index values are consistent with corresponding high values of A_2 in the high-temperature region, implying that synergistic interactions may be triggered by increased A_2 as a result of high concentrations of reactants.[35]

On the basis of the claims that more significant synergistic interactions occurred between biomass or biomass-derived hydrochars and low-rank coals than high-rank coals,[15,36] the results in this study suggest that both synergistic and antisynergistic interactions can take place depending on the blending ratio as well as the intrinsic fuel characteristics of the

dx.doi.org/10.1021/ef501386g | Energy Fuels 2014, 28, 6140−6150

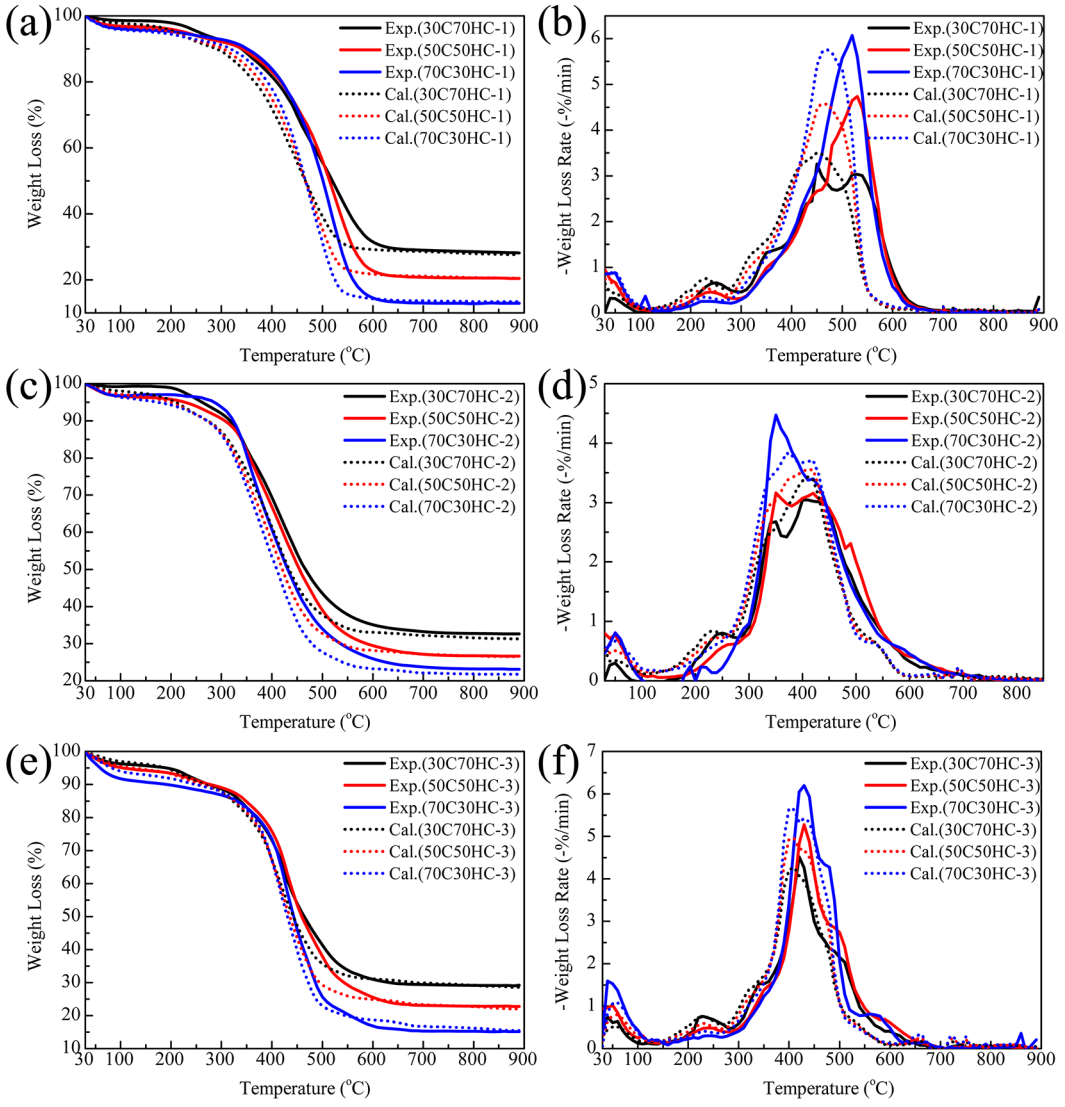

Figure 5. Comparisons of experimental and calculated TG and DTG curves for cocombustion of SHC-320 and different-rank coals at three blending ratios: (a) TG and (b) DTG curves for Coal-1 and SHC-320; (c) TG and (d) DTG curves for Coal-2 and SHC-320; (e) TG and (f) DTG curves for Coal-3 and SHC-320.

Table 5. Deviations of Maximum Weight Loss Rates and Residues of Experimental Curves from Calculated Curves and Corresponding Values of the Synergistic Effect Index

				Deviation (%)		
calculated sample	T_m (°C)	$(dw/dt)_{max}$	residue (%)	$(dw/dt)_{max}$[a]	residue[b]	synergistic effect index[c]
30C70HC-1	450.0	3.51	27.71	−3.1	+1.8	1
50C50HC-1	460.0	4.59	20.56	+4.4	−0.3	4
70C30HC-1	470.0	5.76	13.4	+5.4	−3.7	4
30C70HC-2	410.0	3.43	31.3	−10.5	+4.2	1
50C50HC-2	410.0	3.56	26.5	−9.6	+0.4	1
70C30HC-2	370.0	3.83	21.7	+17.5	+6.5	3
30C70HC-3	410.0	4.26	28.6	+6.3	+2.1	3
50C50HC-3	410.0	4.95	22.1	+6.9	+3.2	3
70C30HC-3	400.0	5.65	15.4	+10.4	−1.9	4

[a]The + and − signs denote positive and negative interactions in cocombustion of blends, respectively. [b]The + and − signs denote negative and positive interactions in cocombustion of blends, respectively. [c]A higher index value denotes greater synergistic effect. Specifically, "4" and "1" indicate most intense synergistic and antisynergistic effects, respectively.

hydrochars and coals. Hence, the coal rank and blending ratio are crucial criteria to be determined before cocombustion with SHC solid fuels. To conclude, for high-rank coals, higher coal percentages (≥50%) in the blends would achieve more synergistic interactions, while low blending ratios (≤30%) may cause severe antisynergistic interactions. For low-rank

dx.doi.org/10.1021/ef501386g | Energy Fuels 2014, 28, 6140−6150

coals, high coal percentages (≥70%) may induce positive interactions but more incomplete combustion, whereas coal percentages less than 50% may not benefit cocombustion. The introduction of moderate-rank coals over a wide range of blending ratios can facilitate synergistic interactions.

4. CONCLUSION

Dewatered sewage sludge (DSS) was directly converted to hydrochars under various subcritical water conditions. The fuel characteristics of the hydrochar derived at 320 °C and 12.0 MPa (SHC-320) outweighed DSS and other hydrochars in terms of highest calorific value, safer T_i, greater heat release in a higher temperature region, and slightly decreased T_b during the shortened combustion process. The introduction of SHC-320 lowered the activation energy to initiate main decomposition of coal blends. Moreover, lower amounts of SHC-320 led to a two-stage main cocombustion while larger portions of SHC-320 (≥70%) improved the ignition reactivity of high-rank coal blends. During main cocombustion, blending with SHC-320 resulted in higher heat loss with high-rank coals. Intense synergistic effects were attributed to higher pre-exponential factor values in the second cocombustion stage. At a low coal/SHC-320 ratio (30:70), the highest antisynergistic effects occurred when SHC-320 was blended with low- or high-rank coal, whereas cocombustion with moderate-rank coal was impacted synergistically, resulting in the highest combustion performance and burnout efficiency among the blends.

AUTHOR INFORMATION

Corresponding Authors

*Tel.: +65 6790 4100. Fax: +65 6792 7319. E-mail: che3@e.ntu.edu.sg (C.H.).

*E-mail: jywang@ntu.edu.sg (J.-Y.W.).

Notes

The authors declare no competing financial interest.

ACKNOWLEDGMENTS

The authors acknowledge the Environment Technology Research Program (ETRP Grant 1202-109) under the National Environment Agency of Singapore and the Campus for Research Excellence and Technological Enterprise (CREATE) program under the National Research Foundation of Singapore for financial support. We also thank Ms. Aihong Meng at Department of Thermal Engineering in Tsinghua University for providing coal samples. Chao He thanks Nanyang Technological University for the award of a Ph.D. research scholarship.

REFERENCES

(1) Cao, Y.; Pawłowski, A. *Renewable Sustainable Energy Rev.* **2012**, *16*, 1657−1665.
(2) Manara, P.; Zabaniotou, A. *Renewable Sustainable Energy Rev.* **2012**, *16*, 2566−2582.
(3) He, C.; Chen, C.-L.; Xu, Z.; Wang, J.-Y. *Environ. Technol.* **2014**, *35*, 95−103.
(4) Zhao, P.; Ge, S.; Ma, D.; Areeprasert, C.; Yoshikawa, K. *ACS Sustainable Chem. Eng.* **2014**, *2*, 665−671.
(5) Magdziarz, A.; Wilk, M. *Energy Convers. Manage.* **2013**, *75*, 425−430.
(6) Park, S.-W.; Jang, C.-H. *Waste Manage.* **2011**, *31*, 523−529.
(7) Parshetti, G. K.; Liu, Z.; Jain, A.; Srinivasan, M. P.; Balasubramanian, R. *Fuel* **2013**, *111*, 201−210.
(8) Liu, Z.; Balasubramanian, R. *Bioresour. Technol.* **2013**, *146*, 371−378.
(9) Zhao, P.; Chen, H.; Ge, S.; Yoshikawa, K. *Appl. Energy* **2013**, *111*, 199−205.
(10) He, C.; Giannis, A.; Wang, J.-Y. *Appl. Energy* **2013**, *111*, 257−266.
(11) Idris, S. S.; Rahman, N. A.; Ismail, K. *Bioresour. Technol.* **2012**, *123*, 581−591.
(12) Otero, M.; Gómez, X.; García, A. I.; Morán, A. *Chemosphere* **2007**, *69*, 1740−1750.
(13) Muthuraman, M.; Namioka, T.; Yoshikawa, K. *Bioresour. Technol.* **2010**, *101*, 2477−2482.
(14) Gil, M. V.; Casal, D.; Pevida, C.; Pis, J. J.; Rubiera, F. *Bioresour. Technol.* **2010**, *101*, 5601−5608.
(15) Liu, Z.; Quek, A.; Hoekman, S. K.; Srinivasan, M. P.; Balasubramanian, R. *Bioresour. Technol.* **2012**, *123*, 646−652.
(16) Kurose, R.; Ikeda, M.; Makino, H.; Kimoto, M.; Miyazaki, T. *Fuel* **2004**, *83*, 1777−1785.
(17) Coats, A. W.; Redfern, J. P. *Nature* **1964**, *201*, 68−69.
(18) Wang, C.; Wang, F.; Yang, Q.; Liang, R. *Biomass Bioenergy* **2009**, *33*, 50−56.
(19) Kastanaki, E.; Vamvuka, D.; Grammelis, P.; Kakaras, E. *Fuel Process. Technol.* **2002**, *77*−*78*, 159−166.
(20) Xie, Z.; Ma, X. *Bioresour. Technol.* **2013**, *146*, 611−618.
(21) Liu, Z.; Zhang, F.-S. *Energy Convers. Manage.* **2008**, *49*, 3498−3504.
(22) Liu, N. A.; Fan, W.; Dobashi, R.; Huang, L. *J. Anal. Appl. Pyrolysis* **2002**, *63*, 303−325.
(23) Tahmasebi, A.; Kassim, M. A.; Yu, J.; Bhattacharya, S. *Bioresour. Technol.* **2013**, *150*, 15−27.
(24) Magdziarz, A.; Werle, S. *Waste Manage.* **2014**, *34*, 174−179.
(25) López-González, D.; Fernandez-Lopez, M.; Valverde, J. L.; Sanchez-Silva, L. *Appl. Energy* **2014**, *114*, 227−237.
(26) Vamvuka, D.; Sfakiotakis, S. *Thermochim. Acta* **2011**, *526*, 192−199.
(27) Parshetti, G. K.; Hoekman, S. K.; Balasubramanian, R. *Bioresour. Technol.* **2013**, *135*, 683−689.
(28) Liu, H.-M.; Li, M.-F. *Chem. Eng. Technol.* **2014**, *37*, 95−102.
(29) Xu, C. B.; Lancaster, J. *Water Res.* **2008**, *42*, 1571−1582.
(30) Muthuraman, M.; Namioka, T.; Yoshikawa, K. *Appl. Energ* **2010**, *87*, 141−148.
(31) Zhang, K.; Zhang, K.; Cao, Y.; Pan, W.-p. *Bioresour. Technol.* **2013**, *131*, 325−332.
(32) Liao, Y.; Ma, X. *Appl. Energy* **2010**, *87*, 3526−3532.
(33) Goldfarb, J. L.; Liu, C. *Bioresour. Technol.* **2013**, *149*, 208−215.
(34) Gai, C.; Zhang, Y.; Chen, W.-T.; Zhang, P.; Dong, Y. *Bioresour. Technol.* **2013**, *150*, 139−148.
(35) Xu, C.; Hu, S.; Xiang, J.; Zhang, L.; Sun, L.; Shuai, C.; Chen, Q.; He, L.; Edreis, E. M. A. *Bioresour. Technol.* **2014**, *154*, 313−321.
(36) Moon, C.; Sung, Y.; Ahn, S.; Kim, T.; Choi, G.; Kim, D. *Exp. Therm. Fluid Sci.* **2013**, *47*, 232−240.